Chapter

Cation Exchange Capacity in Grazing Systems and a Case Study for Quantification by Hyperspectral Imaging

Tatiana Rodríguez Monroy, Manuela Ortega Monsalve, Luis Fernando Galeano-Vasco, Marisol Medina-Sierra and Mario Fernando Cerón-Muñoz

Abstract

This chapter provides an overview of cation exchange capacity (CEC) and its importance as an indicator of soil fertility, particularly in the assessment of grassland quality. The limitations of traditional methods are highlighted, and the need to explore more agile approaches to grassland quality assessment is emphasized. The increasing use of hyperspectral information (HSI) as an accurate tool for measuring soil properties, which promotes more effective and sustainable rangeland management, is further explored. This provides data on soil fertility and forage quality, enabling more accurate decisions. The benefits and challenges of using HSI data to estimate CEC and its potential to improve pasture and forage production will also be examined. HSI technology allows information to be collected and analyzed from reflected light at different wavelengths, providing a clear understanding of soil physical and chemical properties. In addition, a case study illustrating the estimation of CIC using hyperspectral cameras in the department of Antioquia, Colombia, is presented. The chapter emphasizes the relevance of this topic in the rangeland context and concludes with a future outlook that anticipates a change in the management and understanding of grazing systems.

Keywords: agriculture, fertility, soil, spectroscopy, supervised algorithms, remote sensing

1. Introduction

The soil is a nonrenewable natural resource that provides essential ecosystem and environmental services. It acts as a support system and nutrient provider for plant growth, supporting food production, and supplying raw materials for a wide range of human activities [1]. To assess the condition and sustainability of the soil, it is necessary to consider its quality, taking into account the integration of chemical, physical, and biological factors [2].

The physical properties of soil are fundamental to understanding its ability to store and release nutrients and to facilitate plant root development. These properties include texture (sand, silt, and clay content), structure (aggregates), porosity (spaces between particles), bulk density, and water holding capacity [3]. Soil respiration, microbial biomass, nitrogen mineralization, and earthworm density are also considered to assess the biological aspects of the soil [4]. On the other hand, soil chemical properties also influence nutrient availability and are essential for plant growth. Among the most important are soil pH, which controls nutrient availability, CEC, which indicates the soil's ability to retain nutrients, and the concentration of primary, secondary, and micronutrients [5].

In this context, soil quality serves as a tool to examine changes caused by soil management practices, such as excessive fertilization, inadequate irrigation, uncontrolled grazing, nutrient depletion through erosion, physical decomposition of aggregates due to over-tillage, loss of organic matter, salinization, and alkalinization [6]. Soil fertility management is one of the most critical decisions as nutrients often limit plant growth and animal performance [5]. Nutrient balances in the grass are crucial in defining fertilization needs when the nutrient balance is negative and in reducing the purchase of off-farm inputs [7]. Therefore, the objective of this chapter is to analyze CEC in grass production and to present a case study for its determination using HSI technology.

2. CEC in grass production and the use of spectra in its estimation

2.1 CEC as an indicator of soil fertility

CEC is a soil property that describes its ability to provide nutrients in the soil solution, making them available for plant uptake. It is a key indicator for assessing soil fertility [8] as it determines the soil's capacity to retain and supply cations essential for healthy plant growth and development. CEC is defined as the sum of exchangeable cations in the soil, including calcium (Ca^{2+}), magnesium (Mg^{2+}), potassium (K^+), sodium (Na^+), hydrogen (H^+), aluminum (Al^{3+}), iron (Fe^{2+}), manganese (Mn^{2+}), zinc (Zn^{2+}), and copper (Cu^{2+}), expressed in $cmol^+kg^{-1}$ or meq/100 g (milliequivalents per 100 grams of soil) [9].

The term "cation exchange" refers to the process by which cations are exchanged in the soil solution, and subsequently absorbed by plant roots. The presence of clay minerals and organic matter (OM) in the soil enhances the amount of cations in the soil solution due to their negative charge, which attracts positively charged ions (cations) to their surfaces through electrostatic forces. As a result, the cations remain within the root zone of the soil (**Figure 1**).

In soil, OM can exhibit CEC by weight that is 4–50 times higher than that of clay. Unlike clay minerals, OM has a distinct negative charge source. This negative charge results from the dissociation of organic acids within OM, resulting in a net negative charge that is balanced by the presence of cations in the soil. This negative charge on OM is referred to as pH-dependent CEC as the dissociation of organic acids is affected by soil pH. Consequently, the actual soil CEC varies as a function of soil pH. For example, a neutral soil with pH 7 containing the same amount and type of OM will have a higher CEC than a soil with a lower pH, such as pH 5 [9]. On the other hand, clay has a high capacity to attract and retain cations due to its chemical structure. The

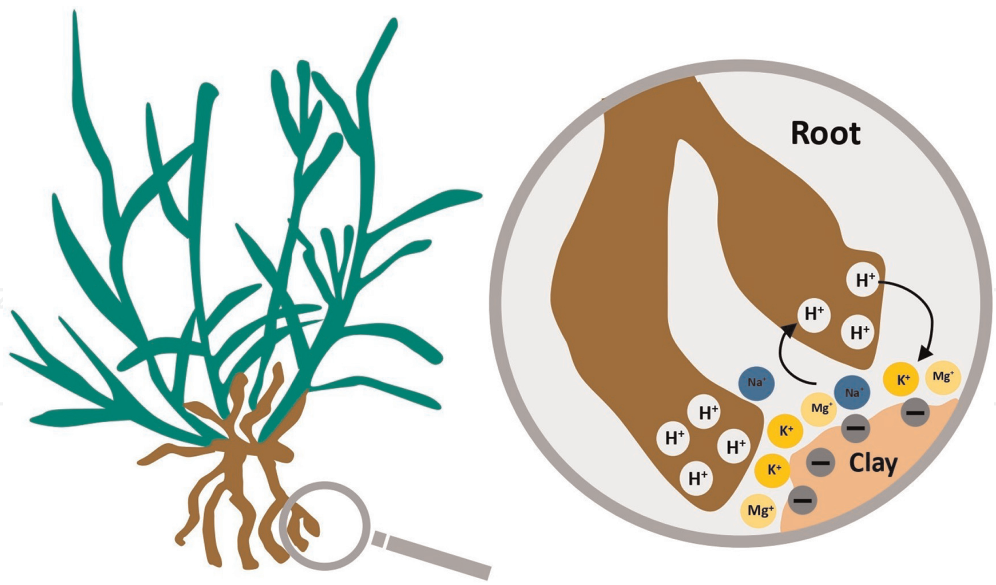

Figure 1.
Cation exchange in the root zone of a grass. Source: Own elaboration.

ratio of CEC to clay content in weight percent can vary significantly because clay minerals exhibit different CECs due to variations in their structure and chemical composition. The proportion of exchangeable cations also varies among different clay minerals. For instance, montmorillonite clay has a higher CEC, heavily weathered kaolinite clay has a lower CEC, and slightly higher CEC is found in the less weathered illite clay [10]. In this context, the estimation of CEC in livestock production systems becomes crucial as it identifies the soil's ability to retain nutrients and provide a favorable environment for pasture growth. By utilizing soil testing techniques, producers can determine the CEC and take appropriate measures to enhance it. This involves the proper application of amendments and fertilizers, adjusting soil pH, and adopting grazing management practices that prevent soil compaction and promote MO incorporation [11]. Improving the soil's CEC ensures the adequate availability of essential nutrients for pasture growth, leading to higher livestock productivity. Moreover, enhancing soil conditions contributes to the conservation of ecosystem structure and health, promoting long-term sustainable management.

2.2 Methods used for the determination of CEC

To quantify CEC and evaluate soil fertility, various direct or conventional methods, as well as indirect or addition methods, have been established. Direct methods involve determining CEC as a single measure by saturating the soil exchange sites with a solution of specific cations, allowing for unique and quantitative measurements. These methods enable CEC determination at different soil pH levels using unbuffered reagents such as KCl, NH_4Cl, and organometallic cations, as well as in a buffered medium to eliminate pH variation in measurements and express all results on the same basis [12]. On the other hand, indirect methods use related parameters, such as exchangeable bases and exchangeable acidity and employ equations to determine CEC. This involves summing up cations and displacing exchangeable cations in the soil using a saturating salt solution, such as ammonium acetate [13].

Currently, the standard reference method most commonly used by laboratories to determine CIC is to saturate the exchange complex with ammonium acetate (1 N at pH 7) for both acidic and alkaline soils. This method uses an ammonium acetate solution to displace the exchangeable cations present in the soil and measures the concentration in the solution to determine the CEC. Another method is the calculation with the sum of exchange bases (Ca^{+2}, Mg^{+2}, K^{+1}, and Na^{+1}). For this process, extraction of 30 to 60 ml of ammonium acetate and 50 ml of 96% ethyl alcohol is required, and for quantification, 50 ml of 10% sodium chloride, 20 ml of formaldehyde, phenolphthalein, and sodium hydroxide are used [14].

The determination of CEC in the laboratory, through direct and indirect methods, presents certain limitations. The preparation of samples, chemical analysis, and interpretation of results requires considerable time, qualified personnel, and specialized equipment. However, a promising alternative for CEC determination is HSI reflectance spectroscopy. This nondestructive technique enables a rapid and efficient analysis of soil, providing detailed information about its properties. By utilizing HSI images, soil reflectance is captured across multiple spectral bands, allowing for the detection of interactions among soil chemical elements. This novel approach has the potential to overcome some of the limitations associated with traditional laboratory methods, facilitating a more precise and detailed assessment of CEC in different soil areas [15].

2.3 Spectroscopy, an alternative to assess soil fertility

The need for faster and more cost-effective analysis has led to the widespread use of infrared spectroscopy. Spectroscopy uses the interaction of light with soil components to provide valuable information about soil properties. The technique is based on measuring the reflection, absorption, and emission of light at different wavelengths to characterize the chemical composition and physical structure of the soil [16]. By analyzing the amount of reflected, absorbed, and transmitted light in each spectral band, detailed data on the different elements and compounds present in the soil can be obtained. This allows a rapid and nondestructive assessment of the chemical and mineralogical composition of the soil, including an estimate of the CEC. This approach reduces the need for traditional laboratory analysis and provides faster results, which can be particularly useful in situations where frequent monitoring of CEC is required over large areas or in resource-limited conditions [17]. It is an emerging technology that successfully predicts the physicochemical properties of soils [15], including CEC, pH, clay content, carbon content, total nitrogen content, and other elements, by correlating spectral data extracted from images with their chemical and physical concentrations [18–20].

This technique is based on the fact that materials reflect electromagnetic energy in the form of different patterns and wavelengths due to their chemical composition, physical structure, and surface properties. HSI captures the radiation reflected from objects in many very narrow spectral bands, creating large data cubes per pixel [21]. The data cubes contain the radiance received by the sensor in a particular band of the spectrum, corresponding to the size of the pixel, which is the smallest visual unit that appears in the image. Each pixel is defined by an integer number known as the digital level (ND). In this sense, the information of an image can be represented as a three-dimensional numerical matrix since it has spatial information on its X and Y axes, corresponding to the geographical coordinates of the image, and spectral information on the Z axis. Considering that HSI images contain a large amount of data, handling, storage, and processing is challenging due to the high spectral variability and correlation in the data. The analysis of large amounts of data involves the following phases:

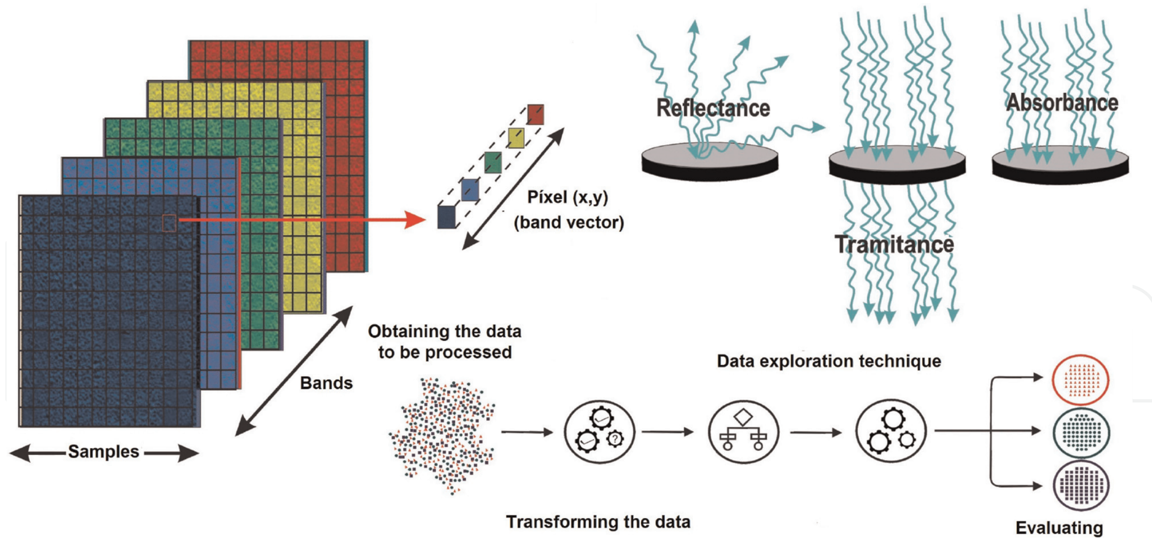

Figure 2.
Hyperspectral information from a hyperspectral image. Adapted from [23].

obtaining the data to be processed, transforming the data so that it can be used, applying the data exploration technique, and evaluating the results obtained [22], as shown in **Figure 2**.

Data transformations are applied to HSI data to reduce noise, improve quality, and enable modeling. Some transformations used for noise removal are the Savitzky-Golay (SG) filter, also known as the digital smoothing polynomial, which reduces the effect of noise without causing much distortion in the spectrum, especially in the width and height of the bands. It is also simple and efficient and involves only a linear convolution with a set of filter coefficients [24]. Another technique used is standard normal variation (SNV) [25], which highlights important patterns and relationships between different bands. On the other hand, the detrending technique (DT) corrects the trend of the data [26].

Similarly, several data exploration techniques have been used to relate the spectra to soil properties and have been used to relate the spectra to soil properties. Among the most widely used are partial least squares regression (PLSR), which can handle large and noisy data sets, and the support vector machine (SVM) method, which is characterized by its ability to generate robust models with few training samples. Other methods, such as artificial neural networks (ANN), are also used in HSI analysis. ANNs consist of an input layer, one or more hidden neuron layers, and an output layer. Decision trees and random forests (RF), which are built from rules, have bifurcations or branches that depend on a condition based on linear regression. These algorithms have been widely used in the scientific literature for the prediction of various soil characteristics using spectral or multidimensional data [27]. Therefore, the aim of this paper is to evaluate supervised learning algorithms in soil CIC estimation from HSI images.

3. Case study

3.1 Generalities

Livestock production is a rapidly growing sector in Colombia. At present, the country's cattle population is spread over 620.807 farms, with a total of 29.642.539

animals, an increase of 1.2% compared to 2022 [28]. This economic activity covers 34 million hectares of land [29], divided into three production systems: dairy, beef, and dual purpose, of which 70% is managed under extensive production systems, with an average stocking density of 0.9 animals per hectare [30].

Livestock diets are based on pasture and forage, with occasional use of concentrates [29]. Although precise data on the range of forage species used in livestock production are not available, it is widely recognized that kikuyu grass (*Cenchrus clandestinus* (Hochst. ex Chiov.) Morrone) plays a crucial role as a forage base in specialized dairy production in high tropical climates [31, 32]. Kikuyu grass is particularly dominant in these areas and provides a constant and abundant source of forage for cattle [33]. In the case of cattle in the mid and low tropics, it has been observed that the most commonly used forage species are star grass (*Cynodon nlemfuensis*), various species of *Brachiaria* (such as *B. decumbens*, *B. humidicola* and *B. brizantha*) and some native species [34].

Livestock productivity is closely linked to the ability of producers to manage their pastures effectively. Proper management involves the accurate and timely application of nutrients necessary for plant growth, which promotes early pasture recovery and maintains sustainable forage production throughout the year [35]. In this sense, a fundamental strategy is to ensure that the soil has the optimum physical and chemical characteristics for adequate plant development. This ensures an environment conducive to the growth of healthy and high-quality grasses.

In the search for faster and more cost-effective alternatives for estimating CEC and assessing soil quality, infrared spectroscopy is emerging as a viable option. This technique provides rapid and nondestructive measurements of soil chemical and mineralogical composition, including CEC estimation, by analyzing the reflection, absorption, and transmission of light at different wavelengths. By using spectroscopy, producers can obtain detailed information on nutrient availability and soil characteristics, enabling them to make informed decisions on nutrient application and pasture management to maximize livestock productivity.

The study area for the estimation of CEC by infrared spectroscopy was located in the department of Antioquia, Colombia, covering the nine subregions and 96 municipalities of the department, as shown in **Figure 3**. The information was obtained from 1997 soil samples collected between November 2020 and November 2022 in pastoral and cocoa production systems. The altitudes of the sampled areas ranged from 0 to 2900 masl and were characterized by a high spatial and temporal variability.

3.2 Methodology

To determine CEC in soil, 1997 samples were analyzed according to the Colombian technical standards NTC 5667:2017 for soil sampling in the field [36] and NTC 5805:2003 for sample preparation for chemical analysis [37]. Laboratory analysis of CEC was carried out at the Colombian Agricultural Research Corporation AGROSAVIA using the indirect method of sum of bases [38].

To record and extract HSI information, HSI images were taken by drying the soil samples at 40°C for 48 hours in a forced-air oven and sieving them at 2 mm. The images were taken using two cameras, the Baldur S-384 N or SWIR (short wave infrared) and the Baldur V-1024 N or VNIR (visible and near infrared). The SWIR camera had a spectral range of 951.61–2517.86 nm, 288 spectral bands, 384 spatial pixels, and a 30 cm lens, while the VNIR camera had a spectral range of 485.14–955.65 nm, 88 spectral bands, 1024 spatial pixels, and a 30 cm lens. Reflectance (R)

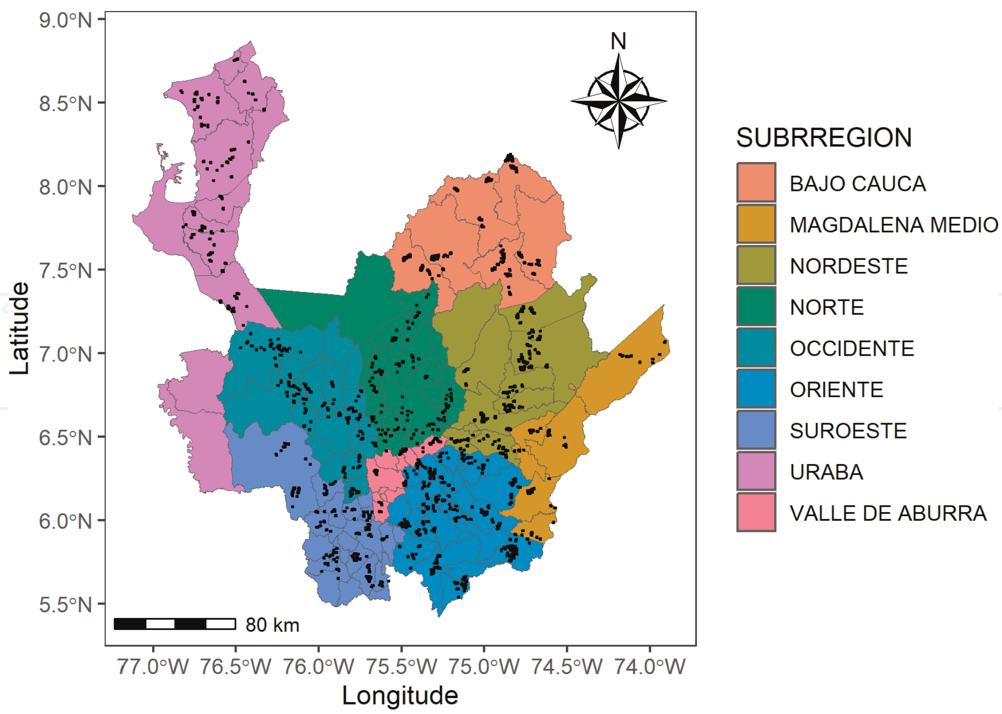

Figure 3.
Location of soil samples collected in the 96 municipalities of the nine subregions of the department of Antioquia.

values were then extracted from the SWIR and VNIR cameras in a region of interest located in the center of the image to avoid pixel errors. Digital masking was applied to pixels with R values greater than 0.2 and less than 0.9 to remove saturated and shaded pixels. This process was performed iteratively using the SpectralPy [39], Spectral [40], and NumPy [41] libraries of the Python 3.8.2 programming language [42].

The overlapping bands detected in the transition region between 950 and 960 nm were removed using the Spectrolab library created by [43] in the R-Project programming language [44]. Band 955 was removed so that the spectra recorded with the VNIR camera ended at band 951, while the SWIR camera started at band 957. Finally, the hyperspectral band database was obtained.

To build the models, the CEC variable was used in its original form and transformed using the Box-Cox method with a value of $\lambda = -0.1547$ and the square root transformation. In addition, the reflectance values were converted to absorbance (ABS) using (Eq. (1)).

$$ABS = log_{10} \frac{1}{R} \tag{1}$$

In addition, SG, SNV, and DT transformations were applied using the prospectr library [45].

PLSR algorithms were applied to these combinations using 5, 10, 15, 20, 25, and 28 components. Each component was constructed by linearly combining the original variables with the intention of maximizing the covariance between the predictor variables and the response variable. SVM models with linear and polynomial kernels were used, with model building costs of 500 and 100, respectively. The data set was divided into training data (train) with 75% of the data and test data (test) with 25% of the data.

To assess the performance and fit of the models, the coefficient of determination (R^2) was used for both the training and test data. In addition, the residual prediction variance (RPD) was calculated. R^2 is obtained by squaring the correlation between the predicted and actual values (Eq. (2)) and provides a measure of how well the model fits the data.

$$R^2 = 1 - \frac{\sum_{i=1}^{n} \left(y_i - \hat{y}_i\right)^2}{\sum_{i=1}^{n} \left(y_i - \bar{y}\right)^2} \tag{2}$$

where:
n : number of observations
y_i : real values
$\hat{y}_i$: values predicted by the model y
$\hat{y}$: mean of the real values

Eq. (3) defines the ratio of performance to deviation (RPD), which is the ratio of the standard deviation of the reference values (observations) to the standard deviation of the differences between the observations and the model predictions. The RPD is a measure used to assess the performance of a predictive model by comparing the accuracy of the reference values with the variability of the model's predictions [46].

$$RPD = \frac{\sqrt{\frac{1}{n-1} \sum_{i=1}^{n} \left(y_i - \bar{y}\right)^2}}{\sqrt{\frac{1}{n} \sum_{i=1}^{n} \left(y_i - \hat{y}_i\right)^2}} \tag{3}$$

3.3 Results and discussion

The CEC values the soils in the department of Antioquia show a wide variability, ranging from a minimum of 0.21 to a maximum of 61.8 cmol (+)/kg. The mean CEC obtained was 8.62 ± 3.33 cmol (+)/kg, with a coefficient of variation of 123.86 cmol (+)/kg. The mode was 0.62 and the median was 33.3 cmol (+)/kg. These results indicate significant variation in CEC across the department, with most samples having low levels of CEC. These results are consistent with previous studies carried out in the northern, northeastern, and Urabá regions of Antioquia [47, 48].

The CEC variable was transformed using the Box-Cox method, resulting in transformed data with a minimum dimension of -1.76 and a maximum dimension of 3.04. The mean obtained after transformation was 1.09 ± 0.99 cmol (+)/kg, with a mode of -0.49 and a median of 1.09 cmol (+)/kg. We also performed the transformation using the square root of CEC, which gave values ranging from a minimum of 0.45 to a maximum of 7.86. The resulting mean was 1.82 ± 1.41 cmol (+)/kg, with a mode of 0.78 and a median of 1.09 cmol (+)/kg. The transformation successfully reduced the scale of the data, as shown in **Figure 4**.

The spectral reflectance of the soil increased as the wavelength increased and remained consistent across different soil samples. Figure illustrates the pattern of the average curves from various samples, displaying several absorption valleys. A reflection peak was observed between 950 and 957 nm, caused by the overlapping noise from VNIR and SWIR sensors, which aligns with the findings described by [49].

The spectral reflectance of the soil increased with wavelength in the visible, near-infrared (NIR) and mid-infrared (MIR) regions, and this behavior was consistent across the different soil samples. A prominent reflection peak was observed between 950 and 957 nm, attributed to the overlapping noise of the VNIR and SWIR sensors,

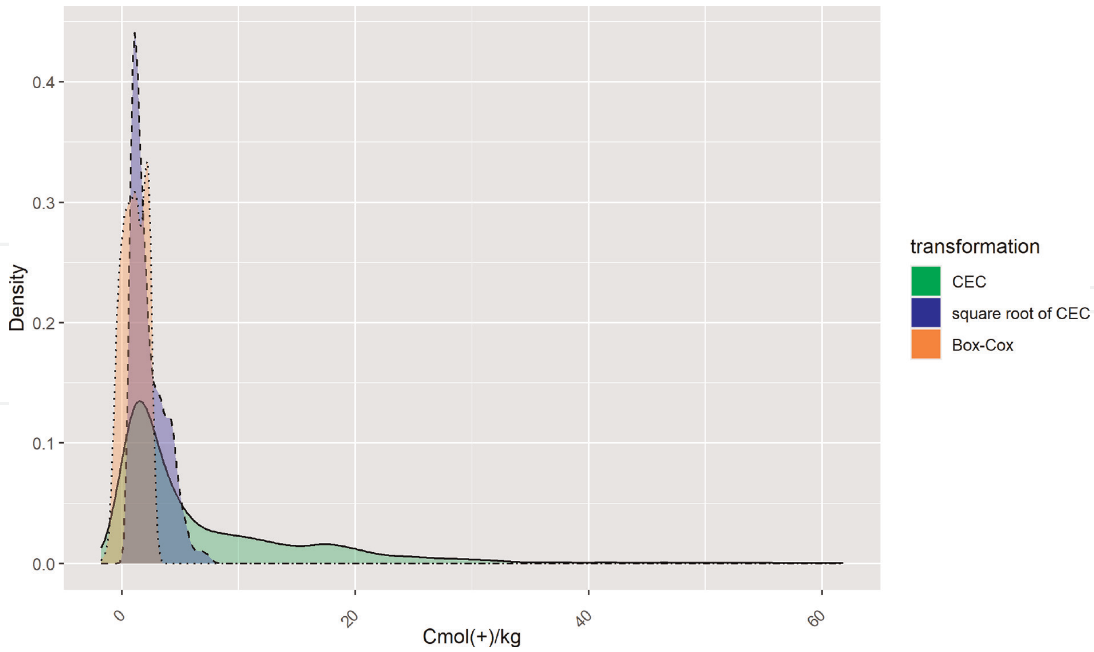

Figure 4.
Diagram of soil CEC distribution, square root, and Box-Cox.

which is consistent with the results described by [49]. In addition, the **Figure 5** illustrates the average curve patterns of the analyzed samples, showing three absorption valleys in the NIR and MIR regions. These observations are consistent with those reported by [50], suggesting that these valleys correspond to the hydroxyl and clay absorption bands of the soils.

A total of 144 PLSR models and 97 SVM models were evaluated for CEC prediction. The PLSR models showed promising results, achieving a RPD_{train} greater than 2, indicating their ability to explain data variability. However, the SVM models outperformed the PLSR models, showing even better performance in explaining data

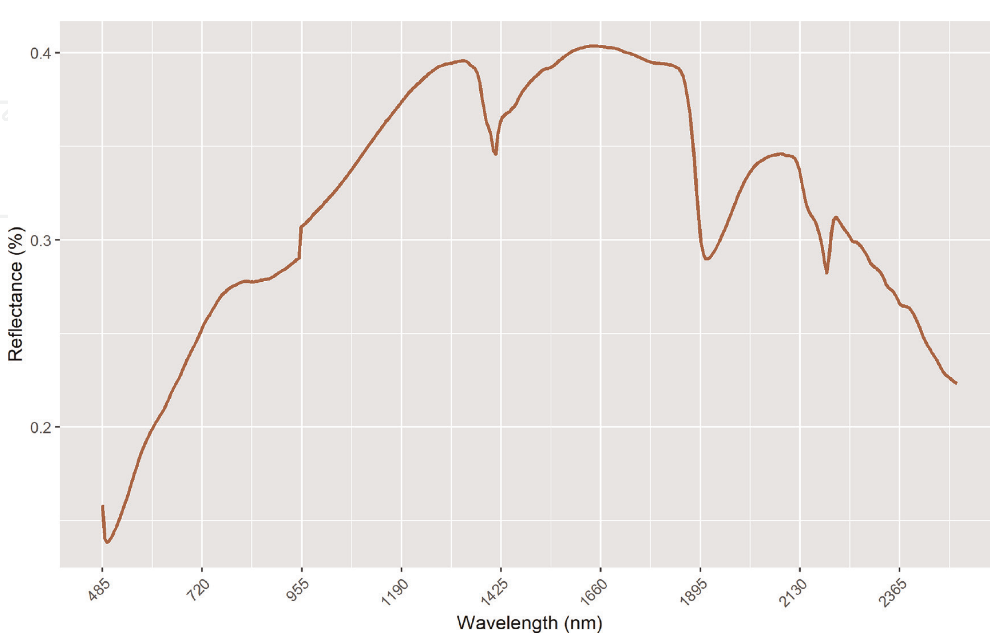

Figure 5.
The spectral signature of the soil.

variability, as evidenced by RPD_{train} and RPD_{test} values greater than 3 and R^2_{train} and R^2_{test} values greater than 0.70. On the other hand, the Kolmogorov-Smirnov (KS) test to assess the goodness of fit test shows that the results obtained for the three best models indicate that the probability distributions of the predicted and observed data adequately fit **Table 1**. These results further support the robustness and quality of the selected SVM models for CEC prediction.

The results obtained in this study are consistent with the findings of [51], who evaluated the predictive ability of the MIR region for CIC (Cation Exchange Capacity). In their research, promising results were obtained using PLSR models, with a coefficient of determination (R^2) of 0.92 and an RPD value of 3.5.

The results reported by [52] agree that SVM models outperformed PLSR models for all soil properties evaluated, including clay, sand, pH, total organic carbon, and permanganate oxidizable carbon, in both training and validation data. These results confirm the relevance and potential of SVM models as a promising option for predicting soil properties from spectral data. Furthermore, the results obtained are in line with the previous study by [53], where they determined the CEC of 142 samples using a spectral range from 350 to 2500 nm. They found a PLSR model with $R^2 = 0.76$ in the training data and $R^2 = 0.72$ in the test data.

On the other hand, it is observed that the models perform better when working with the CEC variable transformed with *sqrtCEC*. As for the HSI data, high performance is obtained with the SNV and DT transformations applied. These results are in line with the results of a study carried out by [41], which showed that preprocessing methods for hyperspectral data improve the accuracy of the evaluated models.

Figure 6 shows a scatter plot comparing the predicted and observed values of the SVM model. The blue dots represent the observed values, while the red dots represent the predicted values. It can be seen that the red dots follow a trend close to the diagonal line, suggesting that the SVM model has effectively captured the variability in the data. It is also important to note that applying the KS test (p-value) to the data yielded values greater than 0.05, indicating that there is no significant difference between the observed and predicted values.

4. Conclusions

In this book chapter, we present promising results in the prediction of the CEC index as an indicator of soil fertility using HSI in the context of pasture production.

Alg.	Variable	Trans	R^2_{train}	R^2_{test}	$\text{RPD}_{\text{train}}$	RPD_{test}	Test KS (p-value)
SVM	$\sqrt{CEC}$	ABS-SNV	0.78	0.79	3.44	3.52	0.44
SVM	$\sqrt{CEC}$	R-SNV	0.78	0.79	3.43	3.51	0.71
SVM	$\sqrt{CEC}$	ABS-DT	0.78	0.77	3.40	3.44	0.46

Alg., Algorithm used for modeling; Variable, conversion method used in the CIC; Trans, data transformation method; train, training data; test, testing data; R^2, coefficient of determination; RPD, ratio of performance to deviation; $TestKS(p - value)$, p-value of the Kolmogorov–Smirnov test; SVM, support vector machines; CEC, cationic interaction capacity; ABS, absorbance; R, reflectance; SNV, standard normal variation; DT, detrending technique.

Table 1.
Results of the five best performing models for predicting cation exchange capacity in the soil.

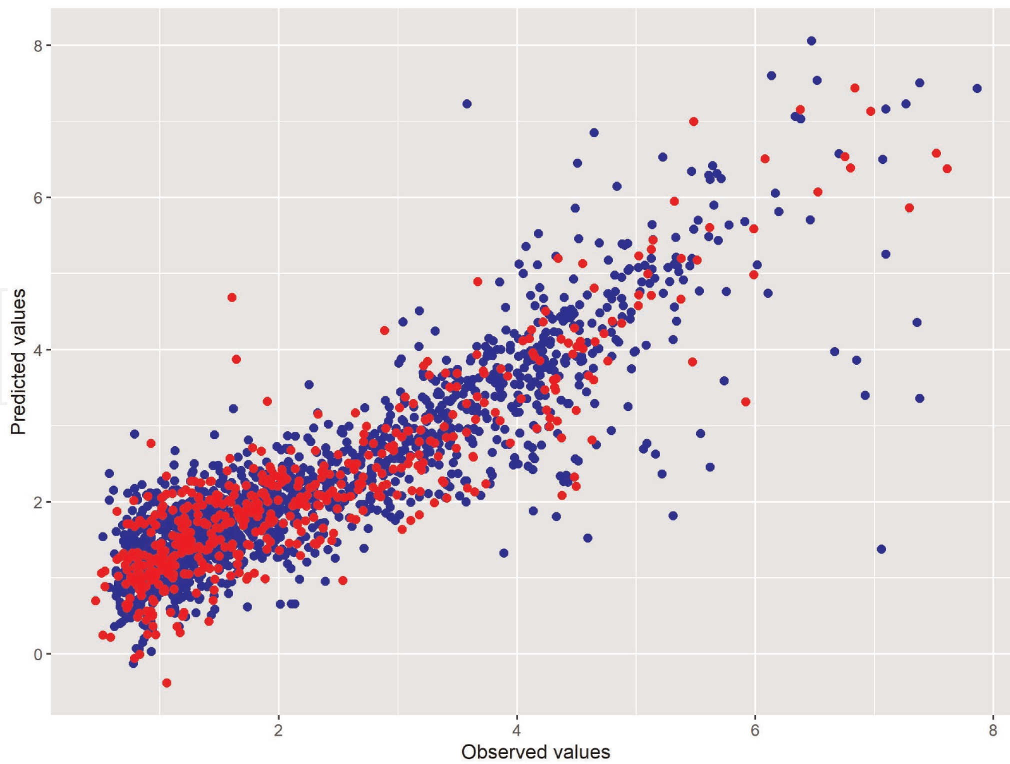

Figure 6.
Observed and predicted values from the SVM model.

The application of HSI technology has shown significant potential for assessing optimal soil conditions and improving management strategies in pasture and forage production. However, it is essential to recognize and address the challenges associated with the use of HSI data in the analysis of soil physicochemical parameters. HSI techniques represent an interdisciplinary field that incorporates and adapts different concepts, approaches, and algorithms. Several signals underline the growing importance of HSI technology in remote sensing. One such indicator is the continuous increase in the number of HSI sensors, supported by the many applications that rely on this technology. In addition, the increase in the number of scientific publications also supports this growth. It is important to note that the methods used to analyze remotely sensed HSI data are not always straightforward. Key challenges include the processing of large amounts of information, high dimensionality, and the need for specialized techniques to extract meaningful patterns and insights. In addition, rigorous data pre-processing and calibration processes are essential to ensure the accuracy and reliability of predictions. One of the most obvious barriers is the management of large data archives, which is hampered by the lack of specialized hardware [27]. As the field of HSI analysis continues to develop, it is imperative that researchers and practitioners develop creative strategies to overcome these barriers and maximize the benefits of HSI technology in soil fertility improvement and pasture production management. Overcoming these challenges will unlock the true potential of HSI technology and usher in a transformative era in soil-related agricultural research and applications. By fully embracing HSI technology and actively addressing its challenges, there is an opportunity to unlock the full potential of hyperspectral data and stimulate positive changes in soil fertility, rangeland productivity, and sustainable agricultural practices.

Acknowledgements

This publication and the financial support of the MSc students was possible thanks to the project "design and validation of predictive models to determine cation exchange capacity (CEC), organic matter (OM), and nitrogen (N) in soils from hyperspectral images" through the agreement 2022-7204, financed by the University of Antioquia Foundation.

Author details

Tatiana Rodríguez Monroy[1*], Manuela Ortega Monsalve[1], Luis Fernando Galeano-Vasco[2], Marisol Medina-Sierra[2] and Mario Fernando Cerón-Muñoz[2]

1 Animal Sciences, GAMMA Research Group, Faculty of Agricultural Sciences, Antioquia University, Medellin, Antioquia, Colombia

2 GAMMA Research Group, Faculty of Agricultural Sciences, Antioquia University, Medellin, Antioquia, Colombia

*Address all correspondence to: tatiana.rodriguezm@udea.edu.co

References

[1] El Burbano-Orjuela H. suelo y su relación con los servicios ecosistémicos y la seguridad alimentaria. Revista de Ciencias Agrícolas. 2015;**33**(2):117-124. DOI: 10.22267/rcia.163302.58

[2] de la Rosa D, Sobral R. Land Use and Soil Resources Chapter Soil Quality and Methods for its Assessment. Dordrecht: Springer; 2008. pp. 167-200. DOI: 10.1007/978-1-4020-6778-59

[3] Cruz A, Barra J, del Castillo RF, Gutiérrez C. La calidad del suelo y sus indicadores. Revista Científica y Técnica de Ecología y Medio Ambiente Ecosistemas. 2004;**13**(2):90-97

[4] Bünemann EK, Bongiorno G, Bai Z, Creamer RE, De Deyn G, de Goede R, et al. Soil quality – A critical review. Soil Biology and Biochemistry. 2018;**120**: 105-125. DOI: 10.1016/j.soilbio.2018.01.030

[5] Silveira ML, Kohmann MM. Maintaining soil fertility and health for sustainable pastures. In: Chapter 3: Management Strategies for Sustainable Cattle Production in Southern Pastures. Florida, United States: Academic Press; 2020. pp. 35-58. DOI: 10.1016/b978-0-12-814474-9.00003-7

[6] Vasu D, Tiwary P, Chandran P, Singh SK. Nutrient dynamics for sustainable crop production. In: Meena R, editor. Chapter: Nutrient Dynamics for Sustainable Crop Production. Singapur: Springer; 2019. pp. 41-66. DOI: 10.1007/978-981-13-8660-22

[7] Dubeux CB, Sollenberger LE. Management strategies for sustainable pastures. In: Chapter 4 - Nutrient Cycling in Grazed Pastures. Florida, United States: Academic Press; 2020. pp. 59-75. DOI: 10.1016/B978-0-12-814474-9.00004-9

[8] García Y, Ramírez S, Sánchez S. Soil quality indicators: A new way to evaluate this resourceIndicadores de la calidad de los suelos: una nueva manera de evaluar este recurso. Pastos y Forrajes. 2012; **35**(2):125-137

[9] Martel YA, De Kipe CR, Laverdiere MR. Cation-exchange capacity of clay-rich soils in relation to organic matter, mineral composition, and surface area. Soil Science Society of America Journal. 1978;**42**(5):764-767

[10] Tan KH, Dowling PS. Effect of organic matter on CEC due to permanent and variable charges in selected temperate region soils. Geoderma. 1984; **32**(2):89-101. DOI: 10.1016/0016-7061(84)90065-X

[11] Noreña GJ. Indicadores de calidad del suelo relacionados con la degradación de la pastura y el rendimiento forrajero del pasto Kikuyo *Cenchrus clandestinus* (Hochst. ex Chiov.) Morrone. Medellín, Colombia: Universidad Nacional de Colombia; 2022

[12] Castillo IA. Comparación de métodos para determinar la capacidad de intercambio catiónico en diez suelos venezolanos. Maracay, Venezuela: Universidad Central de Venezuela; 2019. pp. 27-29

[13] Norman AG, Chapman HD. Methods of Soil Analysis: Part 2 Chemical and Microbiological Properties Chapter 58 Total Exchangeable Bases, Contribution from the Department of Soils and Plant Nutrition. Riverside, CA: University of California; 1995. pp. 902-904. DOI: 10.2134/agromonogr9.2.c7

[14] Instituto Colombiano de Normas Técnicas y Certificación ICONTEC. Gestión ambiental. calidad del suelo.

Pretratamiento de las muestras de suelo para análisis fisicoquímicos NTC-150 11464. Bogotá, DC; 1995

[15] Vargas-Zapata M, Medina-Sierra M, Galeano L, Cerón-Muñoz M. Algoritmos de aprendizaje de máquina para la predicción de propiedades fisicoquímicas del suelo mediante información espectral: una revisión sistemática. Revista de Investigación, Desarrollo e Innovación. 2022;**12**(1):107-120. DOI: 10.19053/20278306.v12. n1.2022.1421

[16] Ferrero A, Frisvad JR, Simonot L, Santafé P, Schirmacher A, Campos J, et al. Fundamental scattering quantities for the determination of reflectance and transmittance. 2021;**29**(1):219-231. DOI: 10.1364/OE.410225

[17] Parody-Zuleta AM, Zapata-Sanjuán ED. Agricultura de precisión en Colombia utilizando teledetección de alta resolución. Suelos Ecuatoriales. 2018;**48**(1):41-49

[18] Lin L, Gao Z, Liu X. Estimation of soil total nitrogen using the synthetic color learning machine (sclm) method and hyperspectral data. Geoderma. 2020;**380**(15):1-10. DOI: 10.1016/j.geoderma. 2020.114664

[19] Guo L, Zhang H, Shi T, Chen Y, Jiang Q, Linderman M. Prediction of soil organic carbon stock by laboratory spectral data and airborne hyperspectral images. Geoderma. 2019;**337**:32-41. DOI: 10.1016/j.geoderma.2018.09.003

[20] Liu L, Ji M, Buchroithner M. Transfer learning for soil spectroscopy based on convolutional neural networks and its application in soil clay content mapping using hyperspectral imagery. Sensors. 2018;**18**(9):1-18. DOI: 10.3390/s18093169

[21] Paoletti ME, Haut JM, Plaza J, Plaza A. Estudio comparativo de técnicas de clasificación de imágenes hiperespectrales. Revista Iberoamericana de Automática e Informática Industrial. 2019;**16**(2):129-137. DOI: 10.4995/riai.2019.11078

[22] Merlino H, Britos PV, Lerache JS, Diez E, García-Martínez R. Un Método de Transformación de Datos Orientado al Uso de Explotación de Información. In: XI Congreso Argentino de Ciencias de la Computación. Buenos Aires, Argentina; 2005

[23] Chuvieco E. Fundamentos de teledetección espacial. Estudios Geográficos. 1991;**52**(203):371

[24] Beitollahi M, Hosseini SA. Using savitsky-golay smoothing filter in hyperspectral data compression by curve fitting. In: 26th Iranian Conference on Electrical Engineering. Mashhad, Irán; 2018. pp. 452-457. DOI: 10.1109/ICEE.2018.8472702

[25] Guo Q, Wu W, Massart D. The robust normal variate transform for pattern recognition with near-infrared data. Analytica Chimica Acta. 1999;**382**(1–2):87-103. DOI: 10.1016/S0003-2670(98)00737-5

[26] Nofrizal AY, Sonobe R, Yamashita H, Mihara M, Morita A, Ikka. Utilization of Hyperspectral Data and Machine Learning Algrorithms for Estimating Chlorophyll Contents in Wasabi Leaves. Vietnam: Universidad de Can Tho, ciudad de Can Tho; 2021

[27] Bioucas-Dias JM et al. Hyperspectral remote sensing data analysis and future challenges. IEEE Geoscience and Remote Sensing Magazine. 2013;**1**(2):6-36. DOI: 10.1109/MGRS.2013.2244672

[28] Instituto Colombiano Agropecuario—ICA. Censos Pecuarios

Nacionales, Censo bovino en Colombia. 2023

[29] Bravo-Parra AM. Cadenas sostenibles ante un clima cambiante. La ganadería en Colombia. Bonn (Alemania). Deutsche Gesellschaft für Internationale Zusammenarbeit (GIZ) GmbH. 2021;**2021**:16-21

[30] Mahecha L. Importancia de los sistemas silvopastoriles y principales limitantes para su implementación en la ganadería colombiana. Revista Colombiana de Ciencias Pecuarias. 2003; **16**(1):11-18

[31] Mojica JE, Castro E, León J, Cárdenas EA, Pabón ML, Carulla JE. Efecto de la oferta de pasto kikuyo *(Pennisetum clandestinum)* sobre la producción y calidad composicional de la leche bovina. Livestock Research for Rural Development. 2009;**21**(1):1-12

[32] Vargas M, Sierra A, Mancipe M, Avellaneda A. El kikuyo, una gramínea presente en los sistemas de rumiantes en trópico alto colombiano. CES Medicina Veterinaria y Zootecnia. 2018;**13**(2): 137-156. DOI: 10.21615/cesmvz.13.2.4

[33] Arango-Gaviria J, Echeverri-Zuluaga J, Lopez-Herrera AC. Diversity Kikuyu grass (*Cenchrus clandestinus*): A review. Journal of Engineering Sciences. 2019; **24**(2):81-88. DOI: 10.22463/0122820X. 1834

[34] Tapasco J, Martínez J, Calderón S, Romero G, Ordóñez DA, Sánchez-Aragón L, et al. Impactos económicos del cambio climático en Colombia: Sector Ganadero. Washington DC: Banco Interamericano de Desarrollo; 2015

[35] Motta-Delgado PA, Martínez O, Rojas-Vargas EP. Indicadores asociados a la sostenibilidad de pasturas: una revisión. Ciencia y Tecnología Agropecuaria. 2019;**20**(2):387-430. DOI: 10.21930/rcta.vol20num2art:1464

[36] Instituto Colombiano de Normas Técnicas y Certificación ICONTEC. NTC 5805:2003: Suelos. preparación de muestras para análisis químico. Norma Técnica Colombiana. 2003

[37] Instituto Colombiano de Normas Técnicas y Certificación ICONTEC. NTC 5667:2017: Suelos. toma de muestras en campo. Norma Técnica Colombiana. 2017

[38] Corporación colombiana de investigación agropecuaria (AGROSAVIA). Informe de analisis químico: Capacidad de intercambio catiónico. Technicalities 2022

[39] Piland R, Frantz D. Spectralpy: A Python Package for Hyperspectral Data Analysis. 2019. Available from: https://github.com/spectralpy/spectralpy

[40] Carriere S, Drumm I. Spectral: Python Package for Hyperspectral Data Analysis. 2021. Available from: https://github.com/spectral/spectral

[41] van der Walt S, Colbert SC, Varoquaux G. Numpy: The Fundamental Package for Scientific Computing with Python. 2011. Available from: https://numpy.org [Accessed: April 7, 2023]

[42] Van Rossum G, Drake FL. Introduction to Python 3: Python. Godalming, England: CreateSpace; 2009

[43] Maughan G, Su J, Ayers L. Spectralab: A Suite of Tools for Spectral Data Analysis in R. 2015. Available from: https://cran.r-project.org/web/packages/SpectraLab/index.html

[44] R Core Team R. A Language and Environment for Statistical Computing.

Vienna, Austria: R Foundation for Statistical Computing; 2023

[45] Malcolm EB, Peter JT, Valkenburgh, BHJ. Tools for Spectroscopy in R. 2019. Available from: https://CRAN.R-project.org/package=prospectr.rpackageversion1.1.7

[46] Wadoux AMC, Malone B, Minasny B, Fajardo M, McBratney AB. Soil Spectral Inference with r. Berlin/Heidelberg, Germany: Springer; 2021. DOI: 10.1007/978-3-030-64896-1

[47] Gordon RAG, Albanes EYA, Sánchez DAC. Evaluación de la calidad química del suelo en agroecosistemas cacaoteros de la subregión del nordeste y Urabá antioqueño. Revista Colombiana de Investigaciones Agroindustriales. 2018;**5**(1):41-52

[48] Sierra-Mediana M, Duque JA, Cerón-Muñoz M. Descripción de las relaciones entre parámetros químicos en suelos de fincas lecheras del norte de antioquia, Colombia. Investigación Ganadera para el Desarrollo Rural. 2019;**31**(7):1-12. DOI: 10.23850/24220582.730

[49] Jin X, Du J, Liu H, Wang Z, Song K. Remote estimation of soil organic matter contentin the sanjiang plain, northest China: The optimal band algorithm versus the GRA-ANN model. Agricultural and Forest Meteorology. 2016;**218–219**:250-260. DOI: 10.1016/j.agrformet.2015.12.062

[50] Streck NA, Rundquist D, Connot J. Spectral signature of selected soils. Revista Brasileira de Agrometeorologia, Santa Maria. 2003;**11**(1):181-184

[51] Lelago A, Bibiso M. Performance of mid infrared spectroscopy to predict nutrients for agricultural soils in selected areas of Ethiopia. Heliyon. 2022;**8**(3):1-6. DOI: 10.1016/j.heliyon.2022.e09050

[52] Deiss L, Margenot AJ, Culman SW, Demyan MS. Tuning support vector machines regression models improves prediction accuracy of soil properties in MIR spectroscopy. Geoderma. 2020;**365**: 114227. DOI: 10.1016/j.geoderma.2020.114227

[53] Wan M, Hu W, Qu M, Li W, Zhang C, Kang J, et al. Rapid estimation of soil cation exchange capacity through sensor data fusion of portable XRF spectrometry and Vis-NIR spectroscopy. Geoderma. 2020;**353**:1-8. DOI: 10.1016/j.geoderma.2019.114163